

Double-pulse characterization by self-referenced spectral interferometry

Cite as: Appl. Phys. Lett. **115**, 051106 (2019); <https://doi.org/10.1063/1.5089959>

Submitted: 24 January 2019 . Accepted: 12 July 2019 . Published Online: 31 July 2019

L. Gulyás Oldal , T. Csizmadia , P. Ye , N. G. Harshitha , M. Füle , and A. Zair 



View Online



Export Citation



CrossMark

ARTICLES YOU MAY BE INTERESTED IN

[Normal dispersion silicon oxynitride microresonator Kerr frequency combs](#)

Applied Physics Letters **115**, 051105 (2019); <https://doi.org/10.1063/1.5096284>

[Phase and amplitude modulation with acoustic holograms](#)

Applied Physics Letters **115**, 053701 (2019); <https://doi.org/10.1063/1.5110673>

[Recent research progress of laser plasma interactions in Shenguang laser facilities](#)

Matter and Radiation at Extremes **4**, 055202 (2019); <https://doi.org/10.1063/1.5092446>

Applied Physics Letters

Mid-IR and THz frequency combs
special collection

[Read Now!](#)

AIP
Publishing

Double-pulse characterization by self-referenced spectral interferometry

Cite as: Appl. Phys. Lett. **115**, 051106 (2019); doi: [10.1063/1.5089959](https://doi.org/10.1063/1.5089959)

Submitted: 24 January 2019 · Accepted: 12 July 2019 ·

Published Online: 31 July 2019



View Online



Export Citation



CrossMark

L. Gulyás Oldal,^{1,a),b)}  T. Csizmadia,^{1,b)}  P. Ye,¹  N. G. Harshitha,¹  M. Füle,¹  and A. Zair^{1,2} 

AFFILIATIONS

¹ELI-ALPS, ELI-HU Non-Profit Ltd., H-6720 Szeged, Hungary

²Department of Physics, King's College, WC2R 2LS London, United Kingdom

^{a)}Electronic mail: lenard.gulyas@eli-alps.hu

^{b)}Contributions: L. Gulyás Oldal and T. Csizmadia contributed equally to this work.

ABSTRACT

The reconstruction of ultrashort optical pulses with a complex intensity substructure is demonstrated using the Self-Referenced Spectral Interferometry (SRSI) pulse characterization technique with a modified phase retrieval algorithm. A correction spectral phase term is extracted by the manipulation of the temporal interferogram, allowing the treatment of scenarios with complicated pulse shapes, where the original algorithm fails. The improved SRSI algorithm is verified through the application on two temporally well-separated pulses having the same polarization direction and spectral shape, generated by duplicating 37 fs-long amplified pulses of a Ti:Sa based laser system. The spectral phase of highly chirped double pulses with equal or different amplitude ratios is numerically retrieved. The collinear and achromatic experimental arrangement results in a compact and easy-to-align system.

Published under license by AIP Publishing. <https://doi.org/10.1063/1.5089959>

Few-cycle laser pulses have already been generated by several research groups^{1–3} allowing the study of ultrafast processes in atoms and molecules^{4–6} and also control chemical reactions.⁷ However, the outcome of these processes, due to their nonlinear nature, strongly depends on the temporal profile of the applied laser pulses. Therefore, the complete (amplitude and phase) temporal characterization of laser pulses is of utmost importance, which has led to the development of dissimilar pulse characterization techniques.^{8–12}

Nowadays, Self-Referenced Spectral Interferometry (SRSI)¹³ is a popular method for determining the time evolution of ultrashort optical pulses. It is based on the interference of an unknown pulse and a self-created reference pulse, which is generated by a third-order nonlinear optical effect.¹⁴ This frequency conserved nonlinear process can be cross-polarized wave (XPW) generation,^{12,15} self-diffraction (SD),^{16,17} or transient-grating (TG) signal production,^{18,19} resulting in an achromatic arrangement. The alignment can also be implemented in a collinear way, making the SRSI setup simple, easily adjustable, and compact in comparison with other well known characterization techniques, such as Frequency-Resolved Optical Gating (FROG)⁹ and Spectral Phase Interferometry for Direct Electric-field Reconstruction (SPIDER).¹⁰ Also, preliminary assumptions regarding the temporal pulse shape are not needed within the phase retrieval algorithm as is required by the FROG technique.

The SRSI pulse characterization method is based on the measurement of the interference between the reference pulse and the delayed unknown laser pulse. An inverse Fourier transform on the measured spectral interferogram results in three well-separated peaks in the time domain. The spectral amplitudes of both the original and the reference pulses can be analytically reconstructed by the numerical filtering of the direct (DC) and alternating (AC) terms and subsequent transformation back to the frequency domain. The spectral phase is retrieved separately by the Gerchberg-Saxton iterative algorithm.²⁰

However, the original SRSI algorithm fails to reconstruct pulses that have a significant intensity substructure. One such example is double pulses with two well-separated temporal peaks, which are represented by distinct frequency bunches in the spectral domain.²¹ Their spectral distance is determined by the temporal separation of the pulses, and the corresponding spectral phase is equivocal. This kind of temporal double-pulse structure is usually used to generate high harmonics using a plasma mirror²² or realize ultrafast pump-probe experiments.²³ Most pulse characterization methods are challenged by such a complicated pulse structure; however, a few techniques have already been developed, such as the improved FROG algorithm²⁴ or the VAMPIRE technique²⁵ to overcome the above-mentioned relative phase ambiguities.²⁶

This letter presents a method, which allows the reconstruction of complex intensity substructures based on the experimentally

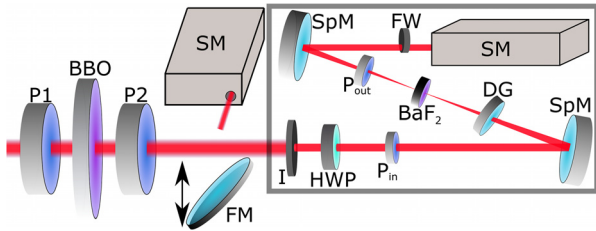


FIG. 1. Schematic of the experimental setup: (P1, P2) polarizers, (BBO) β -Barium Borate crystal, (FM) flip mirror, and (SM) broadband spectrometer. The Wizzler device, used to record the spectral interferograms, consists of an iris (I), a half-wave plate (HWP), two spherical mirrors (SpM), a delay generator (DG), a BaF₂ nonlinear crystal, input and output polarizers (P_{in} , P_{out}), and a filter wheel (FW).

advantageous SRSI technique. This improved SRSI algorithm overcomes the issue of the aforementioned phase ambiguity. We elucidate the introduced modification in the spectral phase, and the theoretical calculations are compared and contrasted with experimentally performed measurements.

Figure 1 shows the experimental arrangement. The spectral interferograms were recorded using commercial pulse characterization equipment based on the XPW-SRSI (WIZZLER, Fastlite Ultrafast Scientific Instrumentation) (gray boxed section in Fig. 1). A temporal double-pulse is generated from an ultrashort laser pulse by using a sequence of a broadband polarizer (P1), a birefringent β -Barium-Borate (BBO) crystal, and another broadband polarizer (P2). The first polarizer transmitted a linearly polarized beam toward the BBO crystal that split it to two orthogonally polarized pulses, the ordinary and the extraordinary ones, with τ time delay between them. τ depends on the thickness and the refractive indices of the birefringent material. The amplitude ratio of the generated pulses is finely tunable by rotating the crystal. A flip mirror (FM) was inserted into the beam in order to record the spectra on a broadband VIS-IR (visible-infrared) spectrometer (Ocean Optics HR4000, SM) before the beam goes into the SRSI device.

The proposed modification of the original SRSI algorithm involves the modulation of the inverse-Fourier transformed spectral interferogram [Fig. 2(a) red]. The measured interferogram can be

described as $\tilde{S}(\omega) = \tilde{S}_0(\omega) + \tilde{f}(\omega)e^{i\omega\tau_d} + c.c.$, where $\tilde{S}_0(\omega)$ is the DC, $\tilde{f}(\omega)$ is the AC term of the spectral interferogram, and τ_d is the delay between them.²⁷ In the case of a double-pulse form, the temporal AC and DC components can be written as

$$\tilde{f}(t) = \sum_{k=0,+,-} f_k(t) + c.c., \quad \tilde{S}_0(t) = \sum_{k=0,+,-} S_k(t) \quad (1)$$

[Fig. 2(b)]. The temporal separation between the consecutive $f_k(t)$ terms [or the $S_k(t)$ terms] represents the temporal separation of the double pulses, while the amplitude ratio can be extracted by simple numerical modifications using these terms. The first step of this procedure involves shifting the positive AC terms and their complex conjugates to the position of the DC term and adding them together [Fig. 2(b)], and therefore, an alternated temporal interferogram $G_k(t) = S_k(t) + f_k(t + \tau_d) + c.c.$ can be calculated [Fig. 2(c)]. The peak $G_-(t)$ is then moved in time to overlap with the corresponding positive peak $G_+(t)$ and summarized [Fig. 2(d)]: $S_{mod}(t) = G_0(t) + G_+(t) + G_-(t - 2\tau)$.

Applying the Fourier transform on the resulting $S_{mod}(t)$ interferogram, the spectral phase with edgy and precipitous jumps (φ_{corr}) can be extracted without higher-order dispersions. The higher-order terms (φ_{iter}) are obtained using the Gerchberg-Saxton iteration algorithm,^{20,27} assuming that the two composing pulses have the same phase (not including the carrier envelope phase (CEP)). The final phase (φ_{calc}) is produced by adding the two spectral phase terms together: $\varphi_{calc} = \varphi_{iter} + \varphi_{corr}$. To get better insight into the behavior of the different algorithms, Fig. 3 shows the simulated double-pulse spectrum and four phase terms at different amplitude ratios: the output phase of the original Gerchberg-Saxton algorithm (φ_{iter} —dashed red), the output phase of the improved algorithm (φ_{calc} —solid black), the correction term of the improved algorithm (φ_{corr} —solid green), and the phase to be retrieved (φ_{expd} —solid yellow). For temporal double-pulse, as their amplitude ratio is more and more comparable [Figs. 3(a)–3(c)], the spectral valleys deepen in the spectrum, and edgy and precipitous jumps appear more prevalently in the spectral phase. As shown by the dashed red curve, the original algorithm can retrieve only continuous phase curves. Therefore, the original method cannot

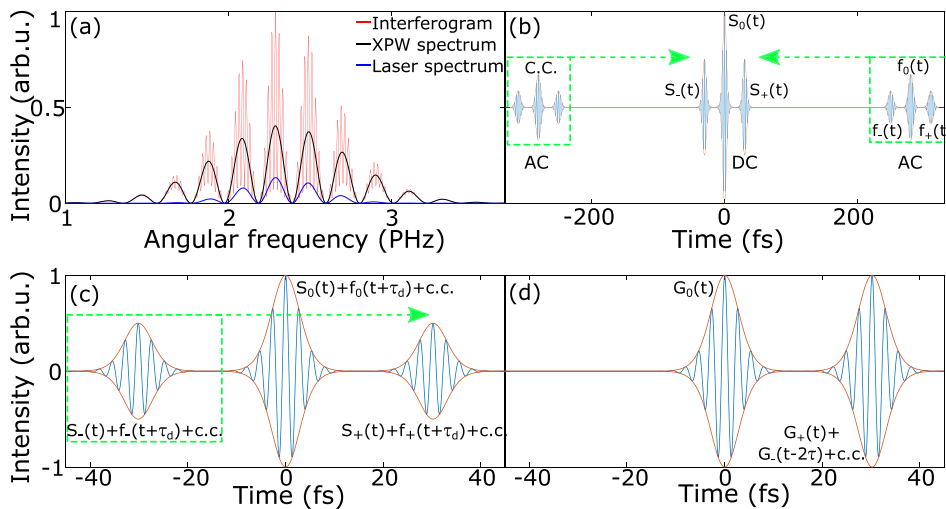


FIG. 2. Steps to calculate the numerical spectrum to extract the correction term of the retrieved spectral phase. (a) Interferogram (red) with the XPW (black) and the laser spectrum (blue). (b) Shifting of the AC terms to overlap with the DC term. (c) Moving of the negative peak to overlap with the positive one. (d) Temporal shape of the modified Fourier-transformed spectral interferogram.

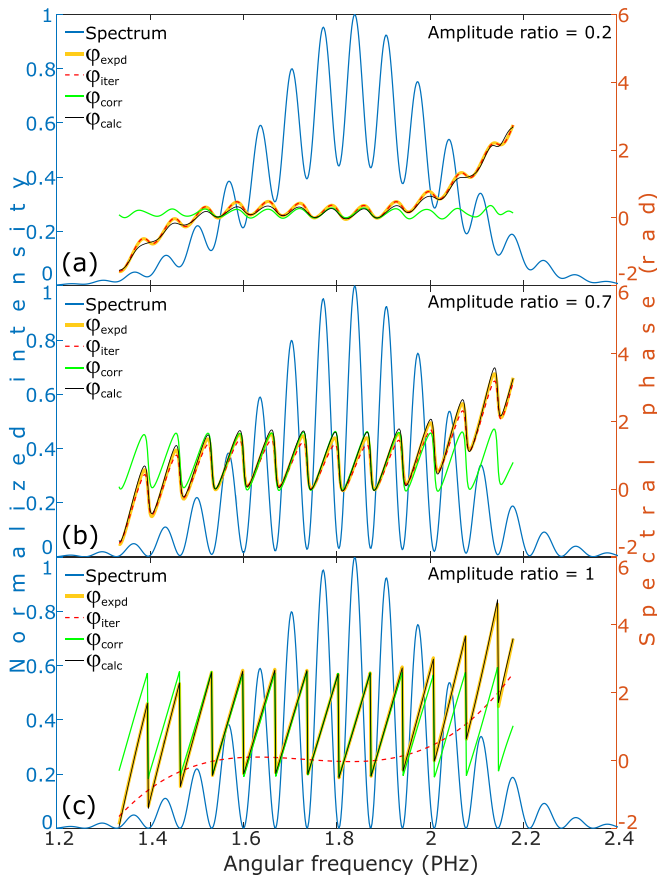


FIG. 3. Spectra (solid blue) and the expected spectral phase (solid yellow), the outcome of the Gerchberg-Saxton iterative algorithm (red dashed), the phase correction term (solid green), and the retrieved spectral phase of double pulses at amplitude ratios of 0.2 (a), 0.7 (b), and 1 (c) applying the improved algorithm (solid black).

retrieve this kind of phase; however, the tendency of the curve inherits the dispersion terms, which can still be properly reconstructed by using the original method. Essentially, φ_{corr} contains the pulse separation and the amplitude ratio property of the double pulses and φ_{iter} provides information about the dispersion terms. By shifting the AC terms to the position of the DC term and summing them together, the effect of the delay generator in the SRSI method can be eliminated. Thereby, the XPW effect also disappears, and thus, the remaining signal contains information about only Fourier-limited pulses.

The error of the methods can be determined by the formula $(\omega_2 - \omega_1)^{-1} \int_{\omega_1}^{\omega_2} |\varphi_{ret}(\omega) - \varphi_{expd}(\omega)| d\omega$, where the expected and retrieved phase are defined as $\varphi_{expd}(\omega)$ and $\varphi_{ret}(\omega)$, respectively. The expected phase is arbitrarily defined. The deviation of the outcome of original and upgraded techniques from the input phase is presented as a function of the amplitude ratio of the two temporal peaks in Fig. 4. The blue curve with circles shows the initial guess of the iterative algorithm, and the error of the original (orange curve with squares) and the improved (yellow curve with crosses) algorithm are presented as well. This figure shows that the original algorithm is inaccurate when the amplitude ratio is greater than 0.65 and it does not deviate

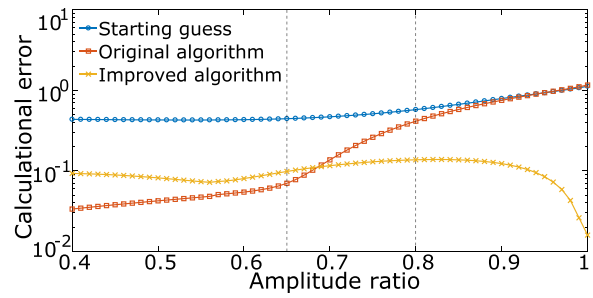


FIG. 4. Deviation from the expected result. The blue curve with circles shows the error of the initial step of the iterative algorithm. The errors of the original and the improved algorithms are shown by the orange curve with squares and the yellow curve with crosses, respectively. Parameters used in the calculation: a laser central wavelength of 1030 nm, a pulse duration of 6.2 fs, a time delay of 92 fs, a group delay dispersion (GDD) of 20 fs², and a third-order dispersion (TOD) of 200 fs³.

significantly from the initial estimate for an amplitude ratio greater than 0.8. By making the modification in the retrieved phase, at the high amplitude ratios, the improved algorithm provides results with substantially smaller error than the original one. Below the amplitude ratio of 0.7, the error of the improved method is higher than the fundamental technique but still less than 10%, which shows the competency of the developed method to adequately reconstruct double pulses at any arbitrary amplitude ratios.

Spectral interferograms were recorded from an arbitrary 0°–90° of the BBO in 5° steps adjusted by a manually rotatable stage. The temporal amplitude, after the second polarizer (*P*₂) of the ordinary ($A_o = A \cdot \cos^2\alpha$) and the extraordinary ($A_e = A \cdot \sin^2\alpha$) pulses, can be calculated using simple geometric considerations. From these expressions, the angle-dependent temporal amplitude ratio of the pulses can be expressed as

$$\frac{A_e}{A_o} = \frac{A \cdot \sin^2\alpha}{A \cdot \cos^2\alpha} = \tan^2\alpha, \quad (2)$$

where α is the angle between the axis of the BBO crystal (\vec{o}) and the polarization direction of the laser beam (\vec{I}). The measured amplitude ratios as a function of the calibrated rotational angles are presented in Fig. 5 (orange dots). A $\tan^2(\alpha + \delta)$ function was fitted (blue curve) on

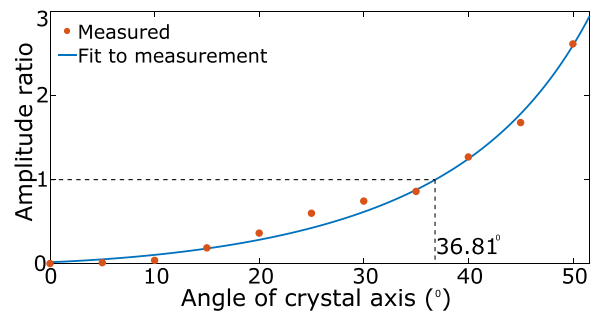


FIG. 5. Measured amplitude ratios (orange dots) of the reconstructed double pulses, calculated by the improved algorithm. The blue line represents the $\tan^2(\alpha + \delta)$ fitting to the experimentally measured amplitude ratios. The indicated value shows the crystal angle, where the pulses are generated with equal amplitudes.

the measured data, where δ is the offset parameter, with which the arbitrary angles of the crystal rotation were subsequently validated. Nevertheless, this technique cannot distinguish the ordinary and the extraordinary pulses, and thus, the maximal amplitude ratio is 1, and after this amplitude ratio, the reciprocal value was calculated and is shown in Fig. 5. The information about the correct sequence of pulses, however, can be gathered by knowing the orientation of the crystal and its direction of rotation during the recording of the data.

Experimental measurements [Figs. 6(c) and 6(d)] and theoretical calculations [Figs. 6(a) and 6(b)] were compared, when the amplitude ratio was higher than 0.7. Experimental measurements were made using the pulses of a Ti:Sa laser system, which spectrum is shown in Fig. 6(c) with a solid blue, with a transform limited duration of 37 fs [Fig. 6(d), solid blue]. The double pulses were generated using a 700 μm thick BBO crystal to introduce a delay of ~ 268 fs between the divided ordinary and the extraordinary pulses. Simulations used a 37 fs length, Gaussian shape pulse and its delayed replica with a 90% amplitude of the original [Fig. 6(b), solid blue] with a delay of 268 fs. The spectral amplitude with the valleys [Fig. 6(a), black line with open circles] and the corresponding complex spectral phase [Fig. 6(a), solid blue] were numerically calculated by applying the Fourier-transform. Higher-order dispersions have not been added to this spectral phase. The results of the phase retrieving using the improved (orange dots) and the original (green dotted line) algorithm are presented in Fig. 6(a), and the related temporal pulse shapes are visible in Fig. 6(b) (orange dots and green

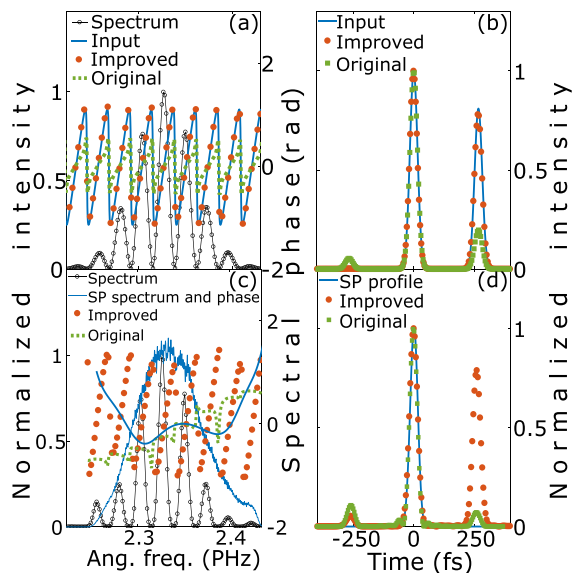


FIG. 6. (a) Spectrum of the simulated double pulses (black line with open circles), the corresponding spectral phase (solid blue), and its retrieval with the improved (orange dots) and with the original (green dotted line) algorithm. (b) The simulated double-pulse (solid blue) and the result of the reconstruction applying the improved (orange dots) and the original (green squares) method. (c) Spectrum of the single-pulse (SP) and the corresponding spectral phase extracted from the WIZZLER apparatus (solid blue), the measured spectral amplitude of double pulses (black line with open circles), the retrieved phase with our algorithm (orange dots), and the outcome of the SRSI device (green dotted line). (d) The corresponding SP shape (solid blue) and double-pulse shapes reconstructed by our algorithm (orange dots) and the result of the SRSI device (green squares).

squares, respectively). The pulse reconstruction from the experimental spectral interferogram is shown in Figs. 6(c) and 6(d). The black curve with open circles shows the recorded spectrum, and the retrieved phase and the reconstructed pulse shape applying the improved algorithm are represented by the orange circles. In Fig. 6(c), the green dotted phase curve was extracted from the SRSI device, and the corresponding pulse shapes are plotted with green squares in Fig. 6(d).

The above results prove the pertinence of the improved algorithm when the pulses are completely separated or their temporal amplitude is different. Nevertheless, the time delay between them is also a key parameter. At short time delays, the density of the frequency component bunches in the spectrum is decreased. Both the original and the improved algorithms provide incorrect results, if there appear only two spectral bunches and one of them is not intense enough. However, in the case of clearly distinguishable spectral bunches, the improved algorithm gives correct outcome, but the original algorithm is still inaccurate. The result of the reconstruction of partially overlapped pulses is presented in Fig. 7.

A final inspection of the techniques was the simulation of adding group delay dispersion (GDD) and third-order dispersion (TOD) to the spectral phase, and 300 fs^2 and 60 000 fs^3 were set, respectively. The other parameters of the simulation were the same as those in Figs. 6(a) and 6(b). Figure 8 shows that the reconstruction of the simulated highly chirped temporal pulse shape matched the original shape well. The high TOD resulted in several low satellites in the temporal profile, but the algorithm could reconstruct the double pulses. In general, similar to the original SRSI algorithm,²⁷ the validity of the reconstruction can be checked by the determination of a broadening coefficient (Z) defined by the ratio of the XPW and the input pulse spectral widths ($Z = \omega_{XPW}/\omega_0$). As a rule of thumb, the measurement is valid as long as $Z > Z_{\text{limit}}$, where $Z_{\text{limit}} = 1$ for Gaussian and $Z_{\text{limit}} > 1$ for super-Gaussian composing pulse forms. It is important to note that even with GDD values slightly larger than the values determined by the broadening criterion, the phase can possibly be recovered; however, the user will not be able to assure the validity of the phase retrieval process in this case.

In conclusion, an upgraded spectral phase retrieval algorithm was demonstrated to improve the SRSI pulse characterization method. The extraction of a correction term of the spectral phase from the manipulated Fourier-transformed spectral interferogram enables the characterization of temporal double pulses having the same spectral

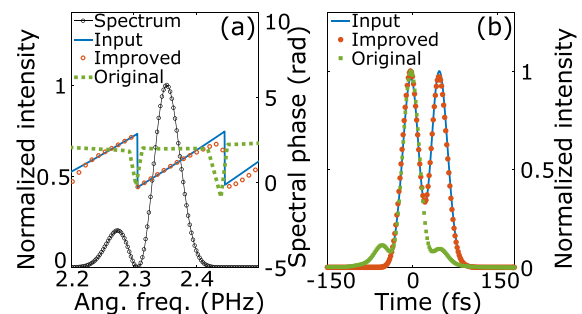


FIG. 7. Reconstruction of temporally overlapped pulses. (a) shows the spectrum (black line with open circles), the input (solid blue) phase, and its reconstruction with the original (green squares) and improved (red open circles) algorithm. The corresponding temporal profiles are presented in (b). The pulse duration is 37 fs, and the delay between them is 45 fs.

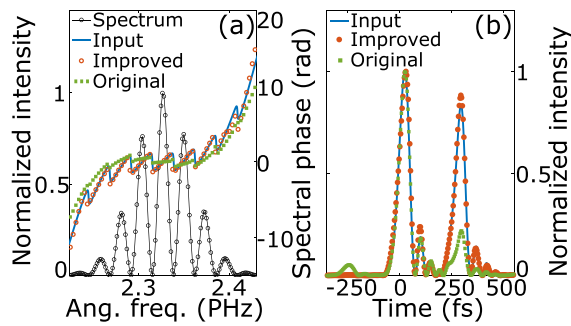


FIG. 8. Temporal profile [(b), solid blue] and the spectral amplitude [(a), black line with open circles] of the simulated double pulses. Simulated spectral phase [(a), solid blue] and its retrieval by the original [(a), green squares] and the improved method [(a), orange open circles] introducing higher-order dispersion. The reconstruction of the temporal shape by the original and the improved algorithm is presented by the green squares and the orange dots in (b), respectively.

amplitude while maintaining the ability to reconstruct simpler spectral shapes. Temporal double pulses are common in laser physics; however, it is not the only pulse form having elaborate intensity behavior that can occur. The reconstruction of this representative case of a complex temporal shape shows that the improved SRSI algorithm, in general, opens up the possibility to reconstruct the temporal envelopes of pulses with an arbitrary intensity substructure, thus enabling better characterization and application of ultrashort light pulses.

We are grateful for the help of Roland Flender and János Csontos at the TeWaTi laboratory of the University of Szeged. This work was financially funded by the ELI-ALPS project (No. GINOP-2.3.6-15-2015-00001), which was supported by the European Union and cofinanced by the European Regional Development Fund. We also acknowledge funding from the Ministry of Human Capacities of Hungary under the Grant “National Programme of Talents,” Application No. NTP-NFTÖ-18-B-0088.

REFERENCES

- ¹R. Budriūnas, T. Stanislaukas, A. Aleknavičius, J. Adamonis, G. Veitas, D. Gadonas, S. Balickas, A. Michailovas, and A. Varanavičius, *Opt. Express* **25**, 5797 (2017).
- ²S. Hädrich, M. Kienel, M. Müller, A. Klenke, J. Rothhardt, R. Klas, T. Gottschall, T. Eidam, A. Drozdy, Z. Várallyay *et al.*, *Opt. Lett.* **41**, 4332 (2016).
- ³N. Thiré, R. Maksimenka, B. Kiss, C. Ferchaud, P. Bizouard, E. Cormier, K. Osvay, and N. Forget, *Opt. Express* **25**, 1505 (2017).
- ⁴T. Zuo, A. D. Bandrauk, and P. B. Corkum, *Chem. Phys. Lett.* **259**, 313 (1996).
- ⁵H. C. Shao and A. F. Starace, *Phys. Rev. Lett.* **105**, 263201 (2010).
- ⁶E. Goulielmakis, Z. H. Loh, A. Wirth, R. Santra, M. F. Kling, N. Rohringer, V. S. Yakovlev, S. Zharebtsov, T. Pfeifer, A. M. Azzeer *et al.*, *Nature* **466**, 739 (2010).
- ⁷A. Assion, T. Baumert, M. Bergt, T. Brixner, B. Kiefer, V. Seyfried, M. Strehle, and G. Gerber, *Science* **282**, 919 (1998).
- ⁸T. D. Jung, F. X. Kärter, J. Henkmann, G. Zhang, and U. Keller, *Appl. Phys. B* **65**, 307 (1997).
- ⁹R. Trebino and D. J. Kane, *J. Opt. Soc. Am. A* **10**, 1101 (1993).
- ¹⁰C. Iaconis and I. A. Walmsley, *Opt. Lett.* **23**, 792 (1998).
- ¹¹L. Gallmann, D. H. Sutter, N. Matuschek, G. Steinmeyer, and U. Keller, *Appl. Phys. B* **70**, S67 (2000).
- ¹²T. Oksenhendler, S. Coudreau, N. Forget, V. Crozatier, S. Grabielle, R. Herzog, O. Gobert, and D. Kaplan, *Appl. Phys. B* **99**, 7 (2010).
- ¹³X. Shen, P. Wang, J. Liu, T. Kobayashi, and R. Li, *Appl. Sci.* **7**, 407 (2017).
- ¹⁴N. Minkovski, G. I. Petrov, S. M. Saltiel, O. Albert, and J. Etchepare, *J. Opt. Soc. Am. B* **21**, 1659 (2004).
- ¹⁵A. Jullien, L. Canova, O. Albert, D. Boschetto, L. Antonucci, Y. H. Cha, J. P. Rousseau, P. Chaudet, G. Chériaux, J. Etchepare *et al.*, *Appl. Phys. B* **87**, 595 (2007).
- ¹⁶J. Liu, K. Okamura, Y. Kida, and T. Kobayashi, *Opt. Express* **18**, 22245 (2010).
- ¹⁷J. Liu, Y. Jiang, T. Kobayashi, R. Li, and Z. Xu, *J. Opt. Soc. Am. B* **29**, 29 (2012).
- ¹⁸J. Liu, K. Okamura, Y. Kida, and T. Kobayashi, *Chin. Opt. Lett.* **9**, 051903 (2011).
- ¹⁹J. Liu, F. J. Li, Y. L. Jiang, C. Li, Y. X. Leng, T. Kobayashi, R. X. Li, and Z. Z. Xu, *Opt. Lett.* **37**, 4829 (2012).
- ²⁰R. W. Gerchberg and W. O. Saxton, *Optik* **35**, 237 (1972).
- ²¹R. Paschotta, *Encyclopedia of Laser Physics and Technology* (Wiley Online Library, 2008), Vol. 1, p. 856.
- ²²C. Thauray, F. Quéré, J.-P. G. A. Levy, T. Ceccotti, P. Monot, M. Bougeard, F. Réau, P. D’oliveira, P. Audebert, R. Marjoribanks *et al.*, *Nat. Phys.* **3**, 424 (2007).
- ²³A. Assion, M. Geisler, J. Helbing, V. Seyfried, and T. Baumert, *Phys. Rev. A* **54**, R4605(R) (1996).
- ²⁴K. W. DeLong and R. Trebino, *J. Opt. Soc. Am. A* **11**, 2429 (1994).
- ²⁵B. Seifert and H. Stolz, *Meas. Sci. Technol.* **20**, 015303 (2009).
- ²⁶D. Keusters, H.-S. Tan, P. O’Shea, E. Zeek, R. Trebino, and W. S. Warren, *J. Opt. Soc. Am. B* **20**, 2226 (2003).
- ²⁷T. Oksenhendler, preprint [arXiv:1204.4949](https://arxiv.org/abs/1204.4949) (2012).